Title	Enhancement of Hotspot Cooling With Diamond Heat Spreader on Cu Microchannel Heat Sink for GaN-on-Si Device
Author(s)	Han, Yong; Lau, Boon Long; Zhang, Xiaowu; Leong, Yoke Choy; Choo, Kok Fah
Citation	Han, Y., Lau, B. L., Zhang, X., Leong, Y. C., & Choo, K. F. (2014). Enhancement of Hotspot Cooling With Diamond Heat Spreader on Cu Microchannel Heat Sink for GaN-on-Si Device. IEEE Transactions on Components, Packaging and Manufacturing Technology, 4(6), 983-990.
Date	2014
URL	http://hdl.handle.net/10220/40786
Rights	© 2014 IEEE. Personal use of this material is permitted. Permission from IEEE must be obtained for all other uses, in any current or future media, including reprinting/republishing this material for advertising or promotional purposes, creating new collective works, for resale or redistribution to servers or lists, or reuse of any copyrighted component of this work in other works. The published version is available at: [http://dx.doi.org/10.1109/TCPMT.2014.2315234].

Enhancement of Hotspot Cooling with Diamond Heat Spreader on Cu Micro-channel Heat Sink for GaN-on-Si Device

Yong Han, Boon Long Lau, Xiaowu Zhang, *Senior Member, IEEE*, Yoke Choy Leong, and Kok Fah Choo

***Abstract*--** The diamond heat spreader has been directly attached between the chip and the Cu micro-channel heat sink for thermal performance improvement of the GaN-on-Si device. In the fabricated test vehicle, the small hotspot is used to represent one GaN unit of several gate fingers. Experimental tests have been implemented on the fabricated test vehicle to investigate the performances. Two types of simulation models have been constructed in COMSOL, considering the multi-physics features and temperature dependent material properties. The sub-model in conjunction with the main model is constructed to predict the thermal performance of the GaN-on-Si structure. The heating power, which is concentrated on the $350\times150\mu m^2$ area, is varied from 10W to 50W. With the diamond heat spreader attached on the liquid-cooled heat sink, the maximum chip temperature can be reduced by 11.5%~22.9%. Consistent results from the experiment and simulation have verified the enhancement of the hotspot cooling capability by using directly attached diamond heat spreader.

***Index Terms*--** Electronic cooling, Micro-channel heat sink, Diamond heat spreader, Heat dissipation capability, Hotspot, High electron mobility transistor (HEMT).

Ⅰ. INRODUCTION

As s modern electronic devices are becoming faster and incorporating more functions, they are simultaneously shrinking in size and weight. These factors suggest significant increases in the packing densities and heat fluxes for the integrated circuits. Effective thermal management will be the key to ensure that these devices perform well with efficiency and reliability [1]. The problem of heat removal is likely to become more severe due to the presence of hotspot, which could lead to much higher heat

flux than the average over the entire chip and make the temperature distribution highly non-uniform, thus diminishing the device performance and adversely impacting reliability. As the heat dissipation concentrates on tiny gate fingers, the operation of GaN high electron mobility transistor HEMT posts huge challenge to thermal management. J.P. Calame [2] performed experimental investigations on the GaN-on-SiC amplifiers, and 4kW/cm^2 heat flux was located to a 1.2×5mm^2 active area of the 5×5mm^2 die. Y.J. Lee [3] developed a Cu micro-channel heat sink for GaN-on-Si device, and more than 10kW/cm^2 heat flux was concentrated on the 350×150μm^2 hotspots of a 7×7mm^2 Si die. The hotspot removal was also analyzed by V. Sahu [4], and a 500×500μm^2 hotspot area of a 1×1cm^2 die was considered, and more than 1kW/cm^2 could be dissipated.

The micro-channel heat sink can dissipate high heat fluxes anticipated in high power electronic devices [5]. A large heat transfer coefficient can be achieved by using the liquid-cooled micro-channel [6-10]. In addition, the coolant can exchange energy effectively with multiples walls within the channel [11, 12]. E.G. Colgan [13] presented a micro-channel cooler and optimized cooler fin for cooling very high power chip, and 300W/cm^2 uniform heat flux was dissipated. To reduce the thermal resistances through the key thermal path, the cooling solution directly attached to the chip was proposed in Ref [14]. The cooling solution of high thermal conductivity will be required to dissipate the concentrated high heat flux in the chip [15]. The heat spreader tends to be a significant mass in the heat sink [16-19]. CVD diamond, of thermal conductivity five times higher than Cu, can be utilized as the heat spreader for microelectronic cooling [20-23]. A. Rogacs [24] conducted the numerical simulation to evaluate the thermal effect of the diamond heat spreader for a small heat source. J.P. Calame [2] conducted the experimental and simulation analysis on the hybrid micro-channel cooler consisting of diamond-on-Si or diamond-on-SiC, and better performances were exhibited than the Si or SiC alone. According to G. Liu's numerical calculations, a thin diamond heat spreader could enable about 10% to 20% decrease of the whole thermal resistance of the heat sink [25].

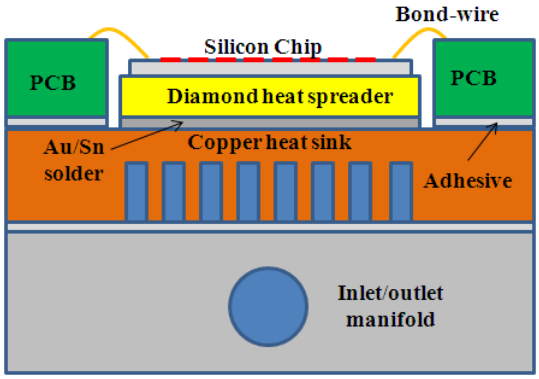

Fig.1 Schamtic image of the cooling structure with diamond heat spreader and liquid-cooled Cu heat sink

In this study, a diamond heat spreader of similar size to the chip has been utilized to enhance the hotspot cooling capability of the liquid-cooled Cu heat sink. The Si test chip, the diamond heat spreader and the Cu micro-channel heat sink are directly bonded together, as is shown in Fig.1. The hotspot (resistor) of tiny area is used to represent the gate finger heating area of the GaN unit. Two types of simulation models, main model of hotspot heating and sub-model of gate finger heating, have been built to investigate the thermal performance. The simulation results show great agreement with the experimental results. The sub-model is used in conjunction with the main model to predict the peak temperature of the transistors under the gate areas. The diamond heat spreader is verified to enhance the heat sink performance by reducing the concentrated high heat flux. Better heat dissipation capability can be achieved by using the directly attached diamond heat spreader for GaN-on-Si device.

II. EXPERIMENT

A top view of the typical GaN-on-Si power amplifier (PA) is shown schematically in Fig.2. There are 8 GaN units in this configuration, and each unit is composed of 10 gate fingers of gate width W_G, gate length L_G and gate-to-gate pitch P_G. The HEMT structure, which is magnified in the inset of the Fig.2, consists of source (S), drain (D) and gate (G). During operation, the vast majority of the waste heat in the GaN PA is generated in the portion of each conductive channel that lies directly beneath the gate finger. The Si substrate die is considered in this study, and 8 GaN units cover 8 rectangular active

regions on top of the die.

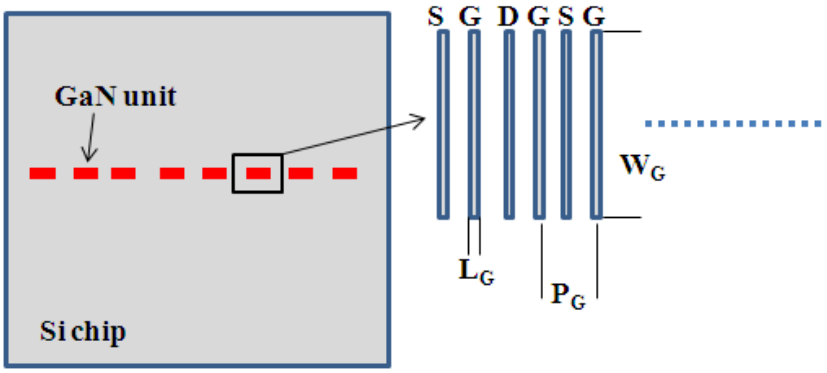

Fig.2 Simplified layout of the GaN-on-Si power amplifier

The experimental tests have been implemented on the Si thermal test chip of 7×7mm^2 size and 200μm thickness with 8 hotspots evenly located in line, as is illustrated in Fig.2. The size of each hotspot is 350×150μm^2, which is a good approximation of an area of 10 gate fingers with 150μm W_G, 0.25μm L_G and 36μm P_G. The space between each hotspot is set to be the same as the GaN unit, which is 690μm. The highly doped N-type resistors are built on the thermal chip as the hotspot heaters. The resistors are fabricated through a series of photolithography, etch and implantation processes. The resistivity measurement of the finished wafers shows good consistency within wafer and between wafers. B. L. Lau [26] provided more details on the customized thermal test chip fabrication processes. The back side of the thermal test chip is metalized with a thin Au/Sn layer (4~5μm thick).The pure Cu heat sink is fabricated with micro-machining process. Channel width, fin width and channel depth of the heat sink are designed at 200μm, 150μm and 1mm, respectively. Channel length is set as 4 mm, centered on the heat sink. 21 micro-channels are deployed only at the regions, where hotspots are present. The diamond heat spreader is prepared by Microwave Plasma Chemical Vapor Deposition (MPCVD). For tight bonding with the chip and the heat sink, the diamond heat spreader is metalized with thin Ti/Pt/Au layer (total thickness around 1μm). The heat spreader is of the similar size to the chip and 300 μm thick. The thermal conductivity of the diamond heat spreader at room temperature is larger than 1800W/mK, and may drop to around 1000W/mK at 200°C. To assemble the test vehicle, all

the components are bonded simultaneously using reflow process, in which the peak temperature is around 230°C. A 50μm thick Au/Sn pre-form solder was employed for Cu heat sink bonding, as is shown in Fig.3 (a). The bonded die-to-heat spreader-to-heat sink structure is illustrated in Fig.3 (c).

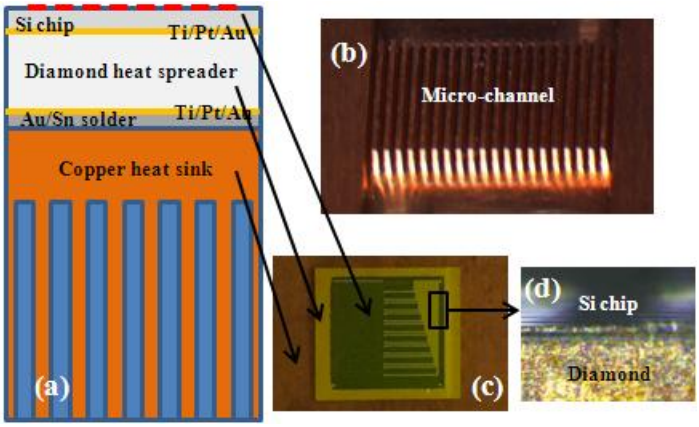

Fig.3 Schematic image of the whole structure (a), image of the fabricated Cu microchannel heat sink (b), topview image of the bonded components (c) and cross-section image of the die-to-diamond bonding (d).

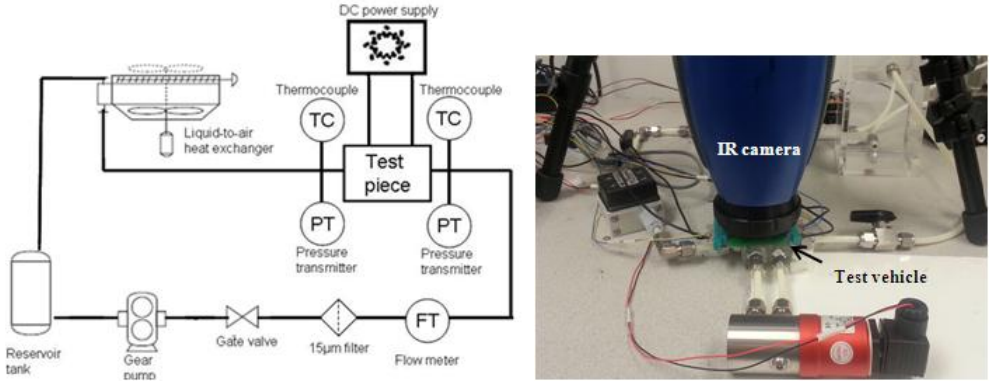

Fig.4. Image of the experimental apparatus

After the fabrication and assembly, the thermal chip was wire bonded to the PCB. The power input to the heaters on the test chip is controlled by a DC power supplier. The experimental apparatus is illustrated in Fig.4. Water, as the coolant, from a reservoir tank is driven through the flow loop using a micro-gear pump. The inlet water and ambient temperature is around 25ºC. This pump forces the water through a 15μm filter and a flow meter before entering the Cu heat sink. The differential pressure transmitter is attached to the manifold to measure the pressure drop. The chip temperature at steady state is measured and recorded using the infrared (IR) camera.

III. SIMULATION

Two types of simulation models are constructed using COMSOL Multi-physics, which runs the finite element analysis together with adaptive meshing and error control. The built-in fluid flow interface and heat transfer interface are used in the main model, which couples both solid and fluid part. Due to the symmetries in the system, a 1/2 of the thermal structure with symmetrical boundary conditions is constructed to investigate the thermal and fluidic performance, as is illustrated in Fig.5. The solution was tested for mesh independency by refining the mesh size. Velocities and temperatures matched within 0.1% for both mesh sizes. The convergence criterion of the solutions is 10^{-6}. The viscous heating feature is considered in the heat transfer interface. The no slip boundary condition is applied for the stationary wall. The model without heat spreader consists of around 1.1 million tetrahedral elements, and the model with heat spreader consists of around 1.25 million. The element size of the fluid part is calibrated for fluid dynamics, while that of the solid part is calibrated for general physics. High heat fluxes are loaded only on the hotspots.

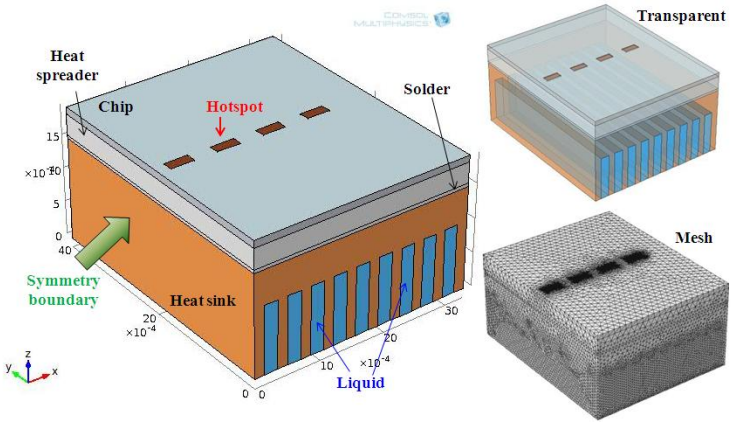

Fig.5 Image of the main model (the fluid part is in blue color) with symmetry boundaries, and the finite element mesh.

As to the GaN unit, the heat producing regions under the gate fingers are much smaller than the chip, which makes it impractical to perform a single detailed simulation of the entire test chip. A sub-model has been constructed to predict the thermal performance of the actual GaN-on-Si device. One GaN unit, which is represented by one hotspot in the main model, is considered in the sub-model,

consisting of 10 gate fingers, and each gate finger is of the size of 150×0.25μm^2. Once the thermal and fluidic performances are computed in the main model, a sub-model is used to compute the peak temperature of the GaN unit. For thermal studies, a number of assumptions were made to limit the scope of the investigation. In the sub-model, the active area of one gate is fixed at 150×0.25μm^2, and all 10 gate fingers in one unit are built considering the heating influences of the nearby gates. The spatially averaged heat transfer coefficients obtained from the main model will be applied to the sub-model as the covective cooling boundaries. Half structure with symmetry boundaries is constructed as is shown in Fig.6. Only the solid parts are considered, and heat transfer coefficient obtained from the main model is applied on the walls of the micro-channl. The model without heat spreader consists of around 0.7 million tetrahedral elements, and the model with heat spreader consists of around 0.8 million. The element size is calibrated for general physics.

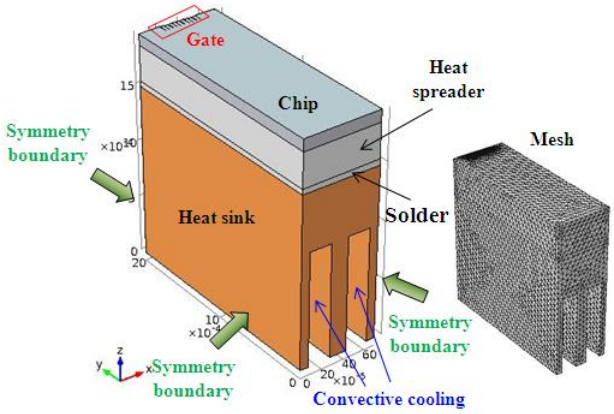

Fig.6 Image of the sub-model with symmetry boundaries, and the finite element mesh.

Ⅳ. RESULTS AND DISSCUSSION

The experimental tests are carried out by heating 8 hotspots simultaneously with 10W~50W total power (heat flux on hotspot:2.38kW/cm^2~11.9kW/cm^2), at the ambient temperature around 25°C. The flow rate of the water across the micro-channel heat sink in this test is set to be 400mL/min, and the pressure drop between the inlet and outlet is around 10kPa. The loading and environment conditions in the simulation are set according to the experimental tests, and temperature dependent material

properties are considered. Based on the estimated low Reynolds number in the heat sink with this flow rate, the micro-channel is considered to be operated in laminar regime. The steady state simulation is performed on the main model. The experimental and simulation results are shown in Fig.7.

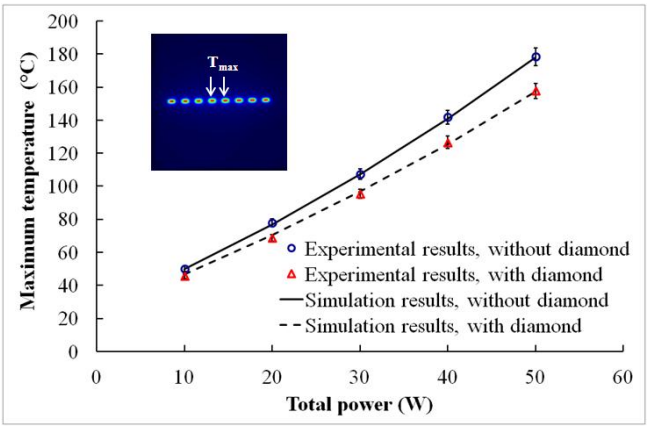

Fig.7 Maximum hotspot temperature as a function of the total heating power for cooling structrure with and without diamond heat spreader from the experimental tests and simulation analysis

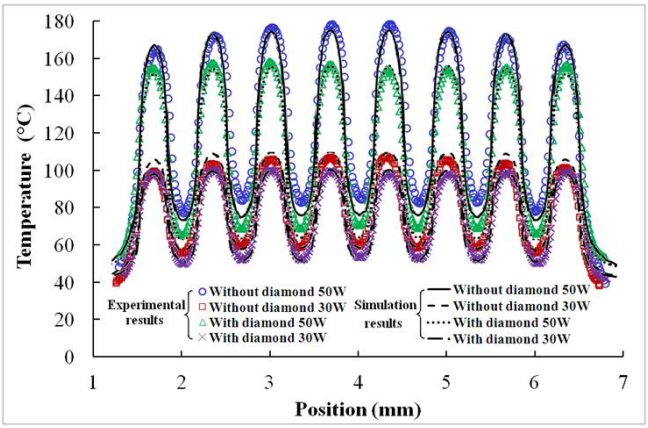

Fig.8 Comparison of the temperature in the thermal chip along the hotspots between experimental tests and simulation analysis for different heat ing power

As is illustrated in Fig.7, excellent agreement has been obtained between experimental results and simulation results. Heated by the same power, the diamond heat spreader can enable round 11.5% decrease of the maximum hotspot temperature of the chip. With the attached heat spreader, 30W, 40W and 50W power can be dissipated, while respectively maintaining the maximum chip temperature under 95ºC, 125 ºC and 160 ºC. The temperature profiles in the longitudinal direction along all hotspots are illustrated in Fig.8. With diamond heat spreader, for 50W power, the maximum

temperature of each hotspot is similar, while without it, there is a 12ºC temperature difference between the hotspots located near the center and near the edge of the chip. The results seen in Fig.7 and 8 shows that, the performances of the structure can be accurately simulated using the main model. Further investigations have been performed based on the simulation results, as is shown in Fig.9 and 10.

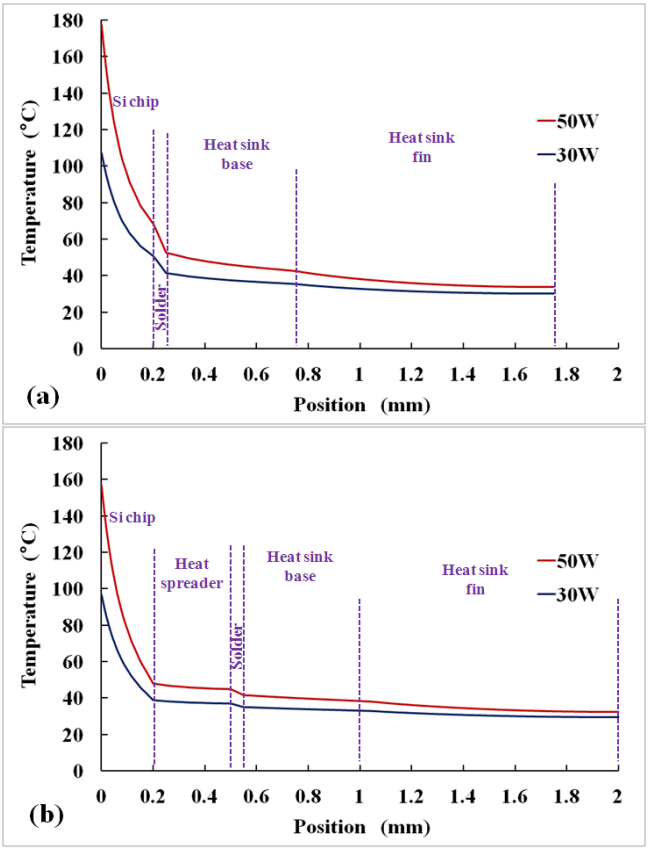

Fig.9 Temperature profie (vertical across the structure for (a) model without diamond heat spreader and (b) with it.

As is shown in Fig.9, lower temperature difference from the chip top to the heat sink top has been achieved by using the diamond heat spreader. The negative effect of the solder layer is weakened. For 50W power, without diamond heat spreader, the temperature difference caused by the solder layer is about 15.7ºC, while that is reduced to 3.2 ºC with diamond. The heat flux on the top surface of the Cu heat sink is quite smaller and more uniform for the cooling structure with diamond than the one without diamond. The results seen in Fig.10 show that the maximum heat flux of model (a) is about1.56kW/cm^2, while that of model (b) is only about 0.35kW/cm^2, suggesting the concentrated heat flux has been reduced to 22.4% by using diamond heat spreader. The maximum thermal resistance of

the whole cooling structure, which is related to the total power and the maximum temperature of the cooling structure, can be reduced by 45.2% with the diamond for the hotspot thermal management.

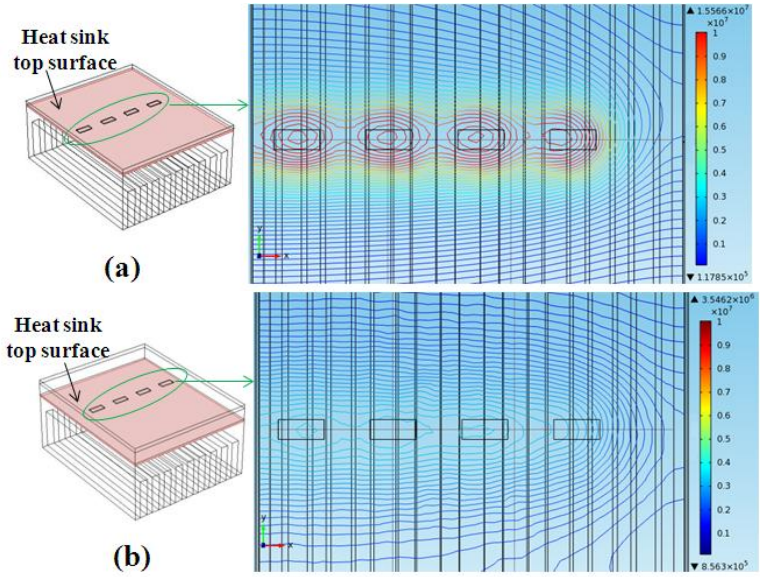

Fig.10 Heat flux distribution on top surface of Cu heat sink for (a) model without diamond heat spreader and (b) with it.

Based on the results from the main model simulation, sub-model in Fig.6 is used to predict the thermal performance of the chip of tiny gate fingers. The interface condition between the main model and the sub-model is the equivalent convective cooling surfaces on the micro-channel walls. The heat transfer coefficient of Cu heat sink is calculated using the equation , in which is the average heat flux, is the average channel wall temperature and is the inlet water temperature. In this study, the heat transfer coefficient is around 4.5×10^{4}W/m^{2}K, and the value is validated by applying it back into the main model shown in Fig.5 without considering the fluid parts. For 50W total power, each GaN device will dissipate 6.25W power, and the heat flux on each gate finger area will be as high as 1.67MW/cm^{2}. The results of the sub-model simulation are shown in Fig.11, which gives the temperature distribution along all gate fingers, compared with the representative hotspot of the main model. The maximum gate temperature of structure (a) is about 250.1ºC, while that of structure (b) is about 227.6 ºC. The diamond heat spreader can enable highly decreased maximum heat flux at the top of the Cu heat sink, and enhances the heat dissipation

capability of the liquid cooling.

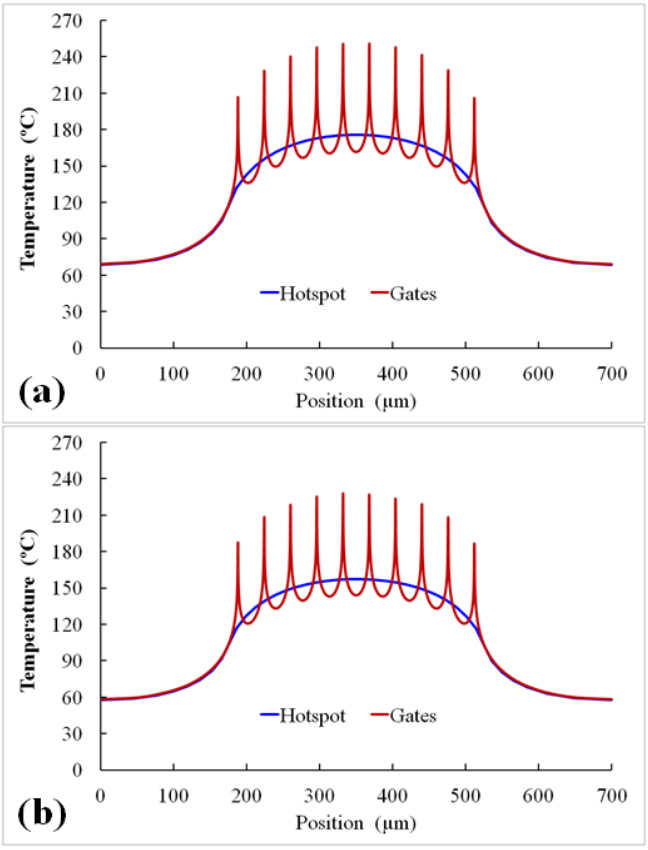

Fig.11 Temperature profile in the longitudinal direction along 10 gate fingers of (a) structure without diamond heat spreader and (b) with diamond heat spreader.

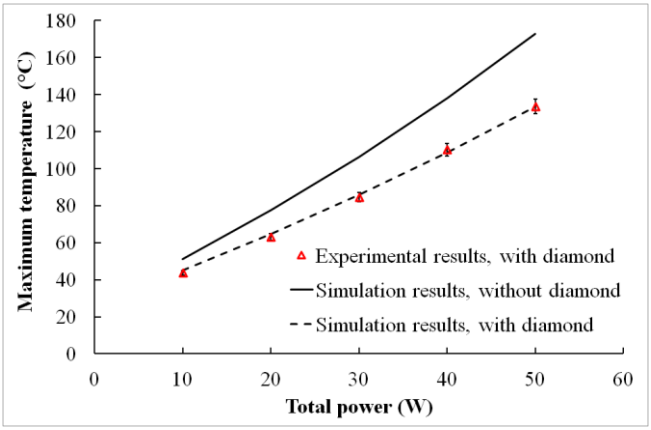

Fig.12 Maximum thin chip temperature as a function of the total power for cooling structrure with and without diamond heat spreader from the experimental tests and simulation analysis

With large concentrated heat flux, the heat transfer capability of the chip can be quite significant in determining the thermal performance. By decreasing the thickness of the Si substrate, the thermal path from the active region to the cooling structure will be shortened, and better thermal performance can

be achieved. The thermal test chip of 100μm thickness was fabricated for further investigations. During the assembly process, the thin Si chips cracked, while being directly bonded with the Cu heat sink under the mentioned reflow bonding conditions, due to the coefficient of thermal expansion (CTE) mismatch. With diamond heat spreader, the thin chip could be bonded with the cooling structure, and no crack was observed in the process. The experimental and simulation results are illustrated in Fig.12. For the structure without diamond heat spreader, only the simulation results are available for comparison.

As is shown in Fig.12, the diamond heat spreader can achieve much better thermal performance, and the improvement is more obvious compared with the results shown in Fig.7. With 50W total power, the diamond heat spreader can enable round 22.9% decrease of the maximum hotspot temperature of the chip. 50W power can be dissipated by the cooling structure with diamond, while maintaining the maximum hotspot temperature under 140ºC. The sub-model simulation is also performed on the thin test chip, and the results are shown in Fig.13. The temperature profile of the main model is shown for comparison. To dissipate 50W, the peak gate finger temperature can be maintained under 200 ºC by using the diamond heat spreader on Cu heat sink cooling solution.

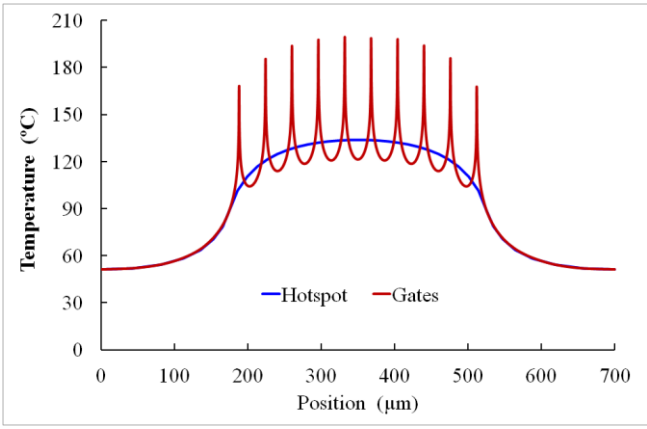

Fig.13 Temperature profile in the longitudinal direction along 10 gate fingers of structurewith diamond heat spreader.

More simulations using the main model have been performed to investigate the effect of the heat spreader thickness on the thermal performance of the structure of 100μm thick chip. The thickness of

the heat spreader is changed from 100μm to 500μm. The variations of the maximum hotspot temperature and the maximum heat flux at the top surface of the Cu heat sink are analyzed, as is illustrated in Fig.14. By increasing the thickness of the heat spreader, the reduced temperature and heat flux can be achieved. The heat spreader used in the tests is 300μm thick, and the thermal performance can be slightly improved by increasing the thickness to 500 μm. The effect is more sensitive by increasing the thickness from 100μm to 300μm, where the maximum temperature and the heat flux can be reduced by around 5.1% and 6.3% respectively.

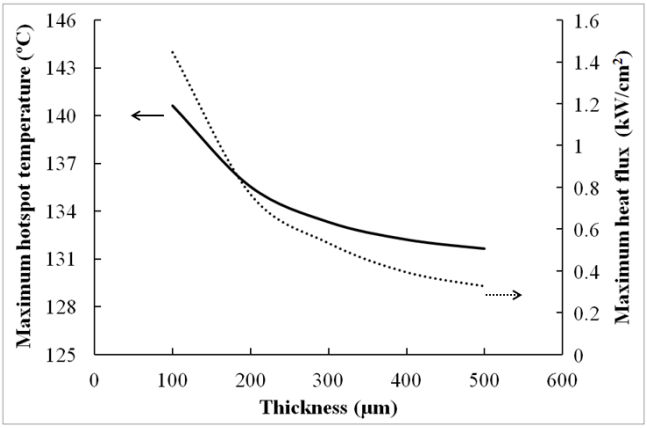

Fig.14 Effect of the heat spreader thickness on the thermal performance of the structure

Ⅴ. CONCLUSIONS

The diamond heat spreader has been bonded together with the Si die and the Cu heat sink for thermal performance improvement. In the fabricated test vehicle, a hotspot of size 350×150 μm^2 is used to represent one GaN unit of 10 gate fingers. High heat flux, from 2.38kW/cm^2 to 11.9kW/cm^2, is concentrated on the heater area in the thermal test chip. Both experimental tests and numerical simulations have been performed to investigate the performances, and consistent results have been obtained. The sub-model in conjunction with the main model is constructed to predict the thermal performance of the GaN-on-Si structure. The maximum temperature of the chip can be highly reduced by using the diamond heat spreader, suggesting more power can be dissipated. For the test chip of

100μm thickness, the diamond heat spreader can enable round 22.9% maximum temperature decrease. 50W power can be dissipated by the cooling structure with diamond, while maintaining the maximum hotspot temperature under 140ºC and the maximum gate finger temperature under 200 ºC. This directly attached diamond heat spreader is verified to enhance the liquid-cooled Cu heat sink performance by effectively spreading the concentrated high heat flux.

ACKNOWLEDGMENT

This work was supported by the Science and Engineering Research Council of A*STAR (Agency for Science, Technology and Research), Singapore, under grant number: 1021740175.

REFERENCES

[1] J. Robinson, " A Thermal–Hydraulic Comparison of Liquid Microchannel and Impinging Liquid Jet Array Heat Sinks for High-Power Electronics Cooling, " IEEE Trans. On CPMT, vol. 32, no. 2, pp. 347-357, June, 2009.

[2] J.P. Calame, R.E. Myers, S.C. Binari, F.N. Wood, and M. Garven, "Experimental investigation of Microchannel Coolers for the High Heat Flux Thermal Management of GaN-on-SiC Semicronductor Devices," Int. J Heat Mass Transfer, Vol. 50, pp. 4767-4779, 2007.

[3] Y. J. Lee, and et al, "GaN-on-Si Hotspot Thermal Management Using Direct-die-attached Microchannel Heat Sink, " 14th IEEE Electronics Packaging Technology Conference, Singapore, pp. 121-125, 2012

[4] V. Sahu, Y.K. Joshi, and A.G. Fedorov, " Energy efficient liquid-thermoelectric hybrid cooling for hot-spot removal", 28th SEMI-THERM, pp.130-134, 2012.

[5] Y. Mizuno, I. Soga, S. Hirose, O. Tsuboi, and T. Iwai, "Si Microchannel cooler Integrated with High Power Amplifiers for Base Station of Mobile Communication Systems", IEEE EPTC, pp. 1541-1546, 2011.

[6] Y. L. Liu, X. B. Luo, and W. Liu, "Experimental Research on a Honeycomb Microchannel Cooling System," IEEE Trans. Compon. Packag. Technol., vol. 1, no. 9, pp. 1378–1386, Sep. 2011.

[7] M. M. Rahman, "Measurements of heat transfer in microchannel heat sinks," Int. Commun. Heat Mass Transfer, vol. 27, no. 4, pp. 495–506, 2000.

[8] H. Y. Wu and P. Cheng, “An experimental study of convective heat transfer in silicon micro channels with different surface conditions,” Int. J. Heat Mass Transf., vol. 46, no. 14, pp. 2547–2556, Jul. 2003.

[9] A. Husain and K. Y. Kim, “Shape Optimization of Micro-Channel Heat Sink for Micro-Electronic Cooling,” IEEE Trans. Compon. Packag. Technol., vol. 31, no. 2, pp. 322–330, May. 2008.

[10] W. Qu, and I. Mudawar, “Experimental and numerical study of pressure drop and heat transfer in a single-phase micro-channel heat sink,” Int. J. Heat Mass. Transf., vol.45, no. 12, pp. 2549–2565, 2002.

[11] D. Liu, and S.V. Garimella, “Analysis and optimization of the thermal performance of microchannel heat sinks,” Int. J. Num. Meth. Heat Fluid flow. vol. 15, no. 1,pp.7–26, 2005.

[12] L. Biswal, S. Chakraborty, and S. K. Son, "Design and Optimization of Single-Phase Liquid Cooled Microchannel Heat Sink," IEEE Trans. on Components and Packaging Technologies, vol. 32, no. 4, pp. 876-886, 2009.

[13] E.G. Colgan, and et al, “A Practical Implementation of Silicon Microchannel Cooler for High Power Chips,” IEEE Trans. On CPT, vol. 30, no. 2, pp. 218-225, 2007

[14] J.P. Calame, R.E. Myers, F. N. Wood, and S.C. Binari, “Simulation of Direct-Die-Attached Microchannel Coolers for the Thermal Management of GaN-on-SiC Microwave Amplifiers,” IEEE Trans. On CPMT, Vol. 28, No. 4, pp. 797-809, 2005.

[15] S. Subrina, D. Kotchetkov, and A.A. Balandin, “Heat removal in Silicon-on-Insultaor Integrated Circuit With Graphene Lateral Heat Spreader,” IEEE Electron Device Letters, vol. 30, No.12, pp, 1281-1283, 2009

[16] G. Maranzana, I. Perry, D. Maillet, S. Rael, “Design optimization of a spreader heat sink for power electronics”, Int. J. Thermal Sciences, Vol. 43, pp. 21-29, 2004.

[17] S. Lee, S. Song, V. Au, and K. P. Moran,“Constriction/Spreading Resistance Model for Electronics Packaging,” Proc. ASME/JSME Thermal Engineering Conference, pp. 111–121, 1994.

[18] T.Q. Feng, J.L. Xu, “An analytical solution of thermal resistance of cubic heat spreaders for electronic cooling”, App. Thermal Engg., Vol. 24, pp. 323-337, 2005.

[19] G.N. Ellison,, “Maximum spreading resistance for rectangular sources and plates with nonunity aspect ratios,”IEEE Transactions on Components and Packaging Technologies, Vol. 26, No. 2, pp. 439-454, 2003.

[20] P. Hui, and H.S. Tan, “Three-dimensional analysis of a thermal dissipation system with a rectangular diamond heat spreader on a semi-infinite copper heat sink,” Jpn. J. Appl. Phys. Vol. 35, pp. 4852-4861, 1996.

[21] P. Hui, and H.S. Tan, “Temperature distributions in a heat dissipation system using a cylindrical diamond heat spreader on a copper heat sink,” Jpn. J. Appl. Phys. Vol. 75, No. 2, pp. 748-757, 1994.

[22] P. Hui, C.P. Tso, and H.S. Tan,“A rigorous series solution for diamond heat spreaders with temperature-dependent thermal conductivity used in microwave power devices,” Jpn. J. Appl. Phys. Vol. 35, No. 11 , pp. 5796-5804, 1996.

[23] K. Jagannadham, “Multilayer diamond heat spreaders for electronic power devices,” Solid-State Electronics Vol. 42, No. 12, pp. 2199-2208, 1998.

[24] A. Rogacs and J. Rhee, “Performance-Cost Optimization of a Diamond Heat Spreader”, Int. Sym. on APM, pp. 65-72, 2007.

[25] G. Liu, and et al, “Design of Micro-Channel Heat Sink with Diamond Heat Spreader for High Power LD”, Int. Sym. on AOMTT, pp.8, 2012.

[26] B.L. Lau, Y.L. Lee, Y.C. Leong, K.F. Choo, X. Zhang, and P/K/ Chan, ”Development of Thermal Test Chip for GaN-on-Si Device Hotspot Characterization,” 14th IEEE EPTC, pp. 746-751, 2012.